Distributive rainfall/runoff modelling to understand runoff to baseflow proportioning and its impact on the determination of reserve requirements of the Verlorenvlei estuarine lake, west coast, South Africa

Andrew Watson[1], Jodie Miller[1], Manfred Fink[2], Sven Kralisch[2,3], Melanie Fleischer[2], and Willem de Clercq[4]

1. Department of Earth Sciences, Stellenbosch University, Private Bag X1, Matieland 7602, South Africa

2. Department of Geoinformatics, Friedrich-Schiller-University Jena, Loebdergraben 32, 07743 Jena, Germany

3. German Aerospace Center (DLR), Institute of Data Science, Maelzerstraße 3, 07745 Jena, Germany

4. Stellenbosch Water Institute, Stellenbosch University, Private Bag X1, Matieland, 7602, South Africa

Keywords: rainfall/runoff modelling, Verlorenvlei reserve, J2000

Abstract

River systems that support high biodiversity profiles are conservation priorities world-wide. Understanding river eco-system thresholds to low flow conditions is important for the conservation of these systems. While climatic variations are likely to impact the streamflow variability of many river courses into the future, understanding specific river flow dynamics with regard to streamflow variability and aquifer baseflow contributions are central to the implementation of protection strategies. While streamflow is a measurable quantity, baseflow has to be estimated or calculated through the incorporation of hydrogeological variables. In

25   this study, the groundwater components within the J2000 rainfall/runoff model were distributed

26   to provide daily baseflow and streamflow estimates needed for reserve determination. The

27   modelling approach was applied to the RAMSAR-listed Verlorenvlei estuarine lake system on

28   the west coast of South Africa which is under threat due to agricultural expansion and climatic

29   fluctuations. The sub-catchment consists of four main tributaries, Krom Antonies, Hol,

30   Bergvallei and Kruismans. Of these, Krom Antonies was initially presumed the largest

31   baseflow contributor, but was shown to have significant streamflow variability, attributed to

32   the highly conductive nature of the Table Mountain Group sandstones and quaternary

33   sediments. Instead, Bergvallei was identified as the major contributor of baseflow. Hol was the

34   least susceptible to streamflow fluctuations due to the higher baseflow proportion (56 %), as

35   well as the dominance of less conductive Malmesbury shales that underlie it. The estimated

36   flow exceedance probabilities indicated that during the 2008-2017 wet cycle average lake

37   inflows exceeded the average evaporation demand, although yearly rainfall is twice as variable

38   in comparison to the first wet cycle between 1987-1996. During the 1997-2007 dry cycle,

39   average lake inflows are exceeded 85 % of the time by the evaporation demand. The

40   exceedance probabilities estimated here suggest that inflows from the four main tributaries are

41   not enough to support Verlorenvlei, with the evaporation demand of the entire lake being met

42   only 35 % of the time. This highlights the importance of low occurrence events for filling up

43   Verlorenvlei, allowing for regeneration of lake-supported ecosystems. As climate change

44   drives increased temperatures and rainfall variability, the length of dry cycles is likely to

45   increase into the future and result in the lake drying up more frequently. For this reason, it is

46   important to ensure that water resources are not overallocated during wet cycles, hindering

47   ecosystem regeneration and prolonging the length of these dry cycle conditions.

1. Introduction

Functioning river systems offer numerous economic and social benefits to society including water supply, nutrient cycling and disturbance regulation amongst others (Costanza et al., 1997; Nelson et al., 2009; Postel and Carpenter, 1997). As a result, many countries worldwide have endeavoured to protect river ecosystems, although only after provision has been made for basic human needs (Gleick, 2003; Richter et al., 2012; Ridoutt and Pfister, 2010). However, the implementation of river protection has been problematic, because many river courses and flow regimes have been severely altered due to socio-economic development (Gleeson and Richter, 2018; O'Keeffe, 2009; Richter, 2010). River health problems were thought to only result from low-flow conditions and if minimum flows were kept above a critical level, the river's ecosystem would be protected (Poff et al., 1997; Tennant, 1976). It is now recognised that a more natural flow regime, which includes floods as well as low and medium flow conditions, is required for sufficient ecosystem functioning (Arthington et al., 2018; Bunn and Arthington, 2002; Olden and Naiman, 2010; Postel and Richter, 2012). For these reasons, before protection strategies can be developed or implemented for a river system, a comprehensive understanding of the river flow regime dynamics is necessary.

River flow regime dynamics include consideration of not just the surface water in the river but also other water contributions including runoff, interflow and baseflow which are all essential for the maintenance of the discharge requirements. Taken together these factors all contribute to the hydrological components of what is called the ecological reserve, the minimum environmental conditions needed to maintain the ecological health of a river system (Hughes, 2001; King and Louw, 1998; Richter et al., 2003). A variety of different methods have been developed to incorporate various river health factors into ecological reserve determination (Acreman and Dunbar, 2004; Bragg et al., 2005). One of the simplest and most widely applied, is where compensation flows are set below reservoirs and weirs, using flow duration curves to

73   derive mean flow or flow exceedance probabilities (e.g. Harman and Stewardson, 2005). This

74   approach focusses purely on hydrological indices, which are rarely ecologically valid (e.g.

75   Barker and Kirmond, 1998; Lancaster and Downes, 2010).

76   More comprehensive ecological reserve estimates such as functional analysis are focused on

77   the whole ecosystem, including both hydraulic and ecological data (e.g. ELOHA: Poff et al.,

78   2010; Building Block Methodology: King and Louw, 1998). While these methods consider that

79   a variety of low, medium and high flow events are important for maintaining ecosystem

80   diversity, they require specific data regarding the hydrology and ecology of a river system,

81   which in many cases does not exist, has not been recorded continuously or for sufficient

82   duration (Acreman and Dunbar, 2004; Richter et al., 2012). To speed up ecological reserve

83   determination, river flow records have been used to analyse natural seasonality and variability

84   of flows (e.g. Hughes and Hannart, 2003). However, this approach requires long-term

85   streamflow and baseflow timeseries. Whilst streamflow is a measurable quantity subject to a

86   gauging station being in place, baseflow has to be modelled based on hydrological and

87   hydrogeological variables.

88   Rainfall/runoff models can be used to calculate hydrological variables using distributive

89   surface water components (e.g. J2000: Krause, 2001; SWAT: Arnold et al., 1998) but the

90   groundwater components are generally lumped within conventional modelling frameworks. In

91   contrast, groundwater models, which distribute groundwater variables (e.g. MODFLOW:

92   Harbaugh et al., 2000; FEFLOW: Diersch, 2002) are frequently set up to lump climate

93   components. In order to accurately model daily baseflow, which is needed for reserve

94   determination, modelling systems need to be setup such that both groundwater and climate

95   variables are treated in a distributed manner (e.g Bauer et al., 2006; Kim et al., 2008).

96   Rainfall/runoff models, which use Hydrological Response Units (HRUs) as an entity of

97   homogenous climate, rainfall, soil and landuse properties (Flügel, 1995; Leavesley and

98   Stannard, 1990), are able to reproduce hydrographs through model calibration (Wagener and

99   Wheater, 2006; Young, 2006). However, they are rarely able to correctly proportion runoff and

100 baseflow components (e.g. Willems, 2009; Hughes, 2004). To correctly determine

101 groundwater baseflow using rainfall/runoff models such as the J2000, aquifer components need

102 to be distributed. This can be achieved using net recharge and hydraulic conductivity collected

103 through aquifer testing or groundwater modelling.

104 To better understand river flow variability, a rainfall/runoff model was distributed to

105 incorporate aquifer hydraulic conductivity within model HRUs using calibrated values from a

106 MODFLOW groundwater model (Watson, 2018). The model was setup for the RAMSAR

107 listed Verlorenvlei estuarine lake on the west coast of South Africa, which is under threat from

108 climate change, agricultural expansion and mining exploration. The rainfall/runoff model used

109 was J2000 as this model had previously been set up in the region and model variables were

110 well established (e.g Bugan, 2014; Schulz et al., 2013). While the estuarine lake's importance

111 is well documented (Martens et al., 1996; Wishart, 2000), the lake's reserve is not well

112 understood, due to the lack of streamflow and baseflow estimates for the main feeding

113 tributaries of the system. The modelling framework developed in this study aimed to

114 understand the flow variability of the lake's feeding tributaries, to provide the hydrological

115 components (baseflow and runoff proportioning) of the tributaries needed to understand the

116 lake reserve. The surface water and groundwater components of the model were calibrated for

117 two different tributaries which were believed to be the main source of runoff and baseflow for

118 the sub-catchment. The baseflow and runoff rates calculated from the model indicate not only

119 that the lake system cannot be sustained by baseflow during low flow periods but also that the

120 initial understanding of which tributaries are key to the sustainability of the lake system was

121 not correct. The results have important implications for how we understand water dynamics in

122 water stressed catchments and the sustainability of ecological systems in these types of

123 environments generally.

2. Study site

125 Verlorenvlei is an estuarine lake situated on the west coast of South Africa, approximately 150

126 km north of the metropolitan city of Cape Town (Fig. 1). The west coast, which is situated in

127 the Western Cape Province of South Africa, is subject to a Mediterranean climate where the

128 majority of rainfall is received between May to September. The Verlorenvlei lake, which is

129 approximately 15 km^2 in size draining a watershed of 1832 km^2, forms the southern sub-

130 catchment of the Olifants/Doorn water management area (WMA). The lake hosts both Karroid

131 and Fynbos biomes, with a variety of vegetation types (e.g Arid Estuarine Saltmarsh, Cape

132 Inland Salt pans) sensitive to reduced inflows of freshwater (Helme, 2007). A sandbar created

133 around a sandstone outcrop (Table Mountain Group; TMG) allows for an intermittent

134 connection between salt and fresh water. During storms or extremely high tides, water scours

135 the sand bar allowing for a tidal exchange, with a constant inflow of salt water continuing until

136 the inflow velocity decreases enough for a new sand bar to form (Sinclair et al., 1986).

137 The lake is supplied by four main tributaries which are Krom Antonies, Bergvallei, Hol and

138 Kruismans (Fig. 2). The main freshwater sources are presumed to be Krom Antonies and

139 Bergvallei, which drain the mountainous regions to the south (Piketberg) and north of the sub-

140 catchment respectfully. Hol and Kruismans tributaries are variably saline (Sigidi, 2018), due

141 to high evaporation rates in the valley. Average daily temperatures during summer within the

142 sub-catchment are between 20-30 ℃, with estimated potential evaporation rates of 4 to 6 mm.d$^-$

143 ^{1} (Muche et al., 2018). In comparison, winter daily average temperatures are between 12-20 ℃,

144 with estimated potential evaporation rates of 1 to 3 mm.d^{-1} (Muche et al., 2018).
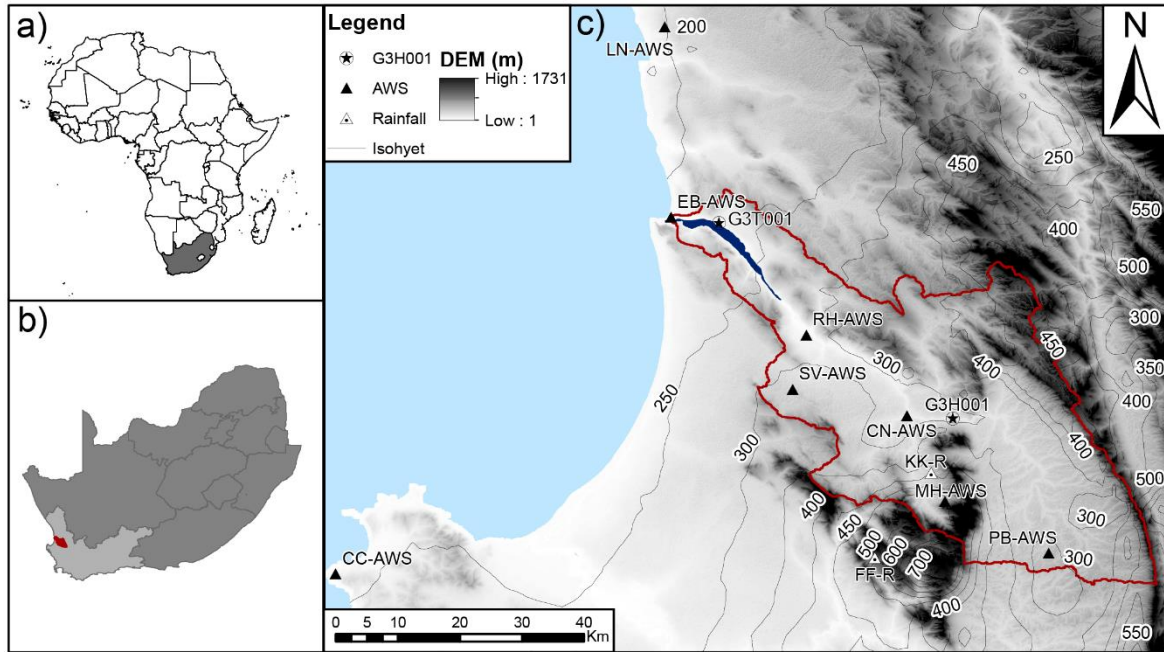
145

146 Figure 1: a) Location of South Africa, b) the location of the study catchment within the Western

147 Cape and c) the extend of the Verlorenvlei sub-catchment with the climate stations, gauging

148 station (G3H001), measured lake water level (G3T001) and rainfall isohyets
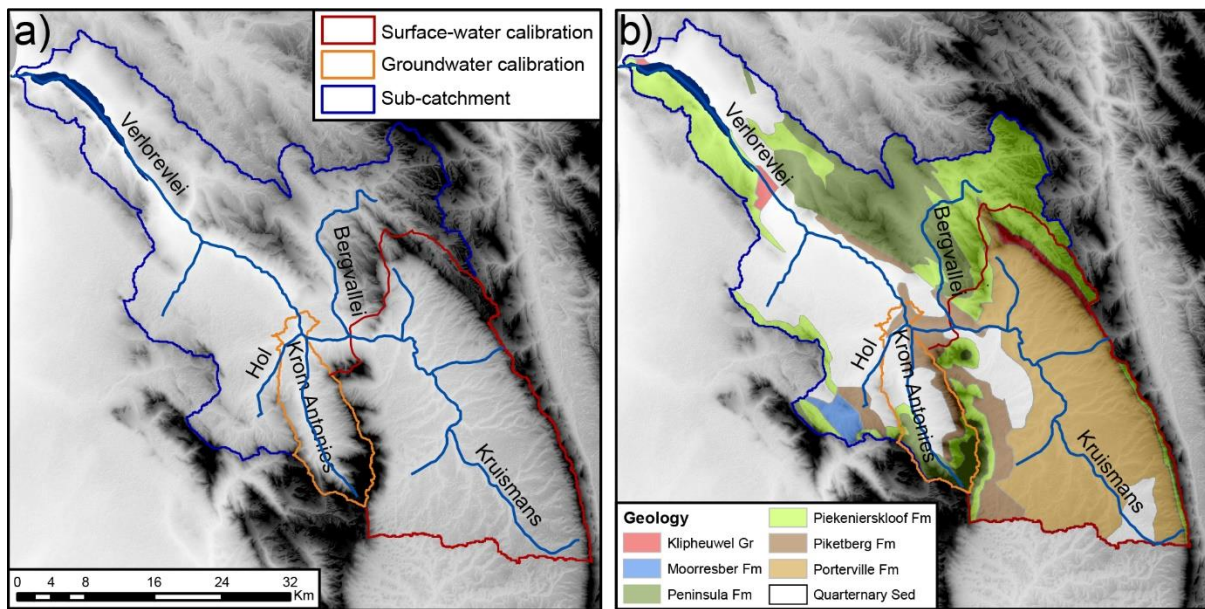
149

150 Figure 2: a) The Verlorenvlei sub-catchment with the surface water calibration tributary

151 (Kruismans) and groundwater calibration tributary (Krom Antonies) and b) the hydrogeology

152 of the sub-catchment with Malmesbury shale formations (MG; Klipheuwel, Mooresberg,

153 Porterville, Piketberg), Table Mountain Group formations (Peninsula, Piekenierskloof) and

154 quaternary sediments

155 Rainfall for the sub-catchment, recorded over the past 52 years by local farmers at KK-R (Fig.

156 1) shows large yearly variability (26 %) between the Mean Annual Precipitation (MAP) (411

157 mm) and measured rainfall (Fig. 3). Where rainfall was greater than 500 mm.yr^{-1} (2006-2010),

158 it is presumed that the lake is supported by a constant influx of streamflow from the feeding

159 tributaries. Recently, where rainfall was less than 50 % of the MAP (2015-2017), concerns

160 over the amount of streamflow required to support the lake have been raised.
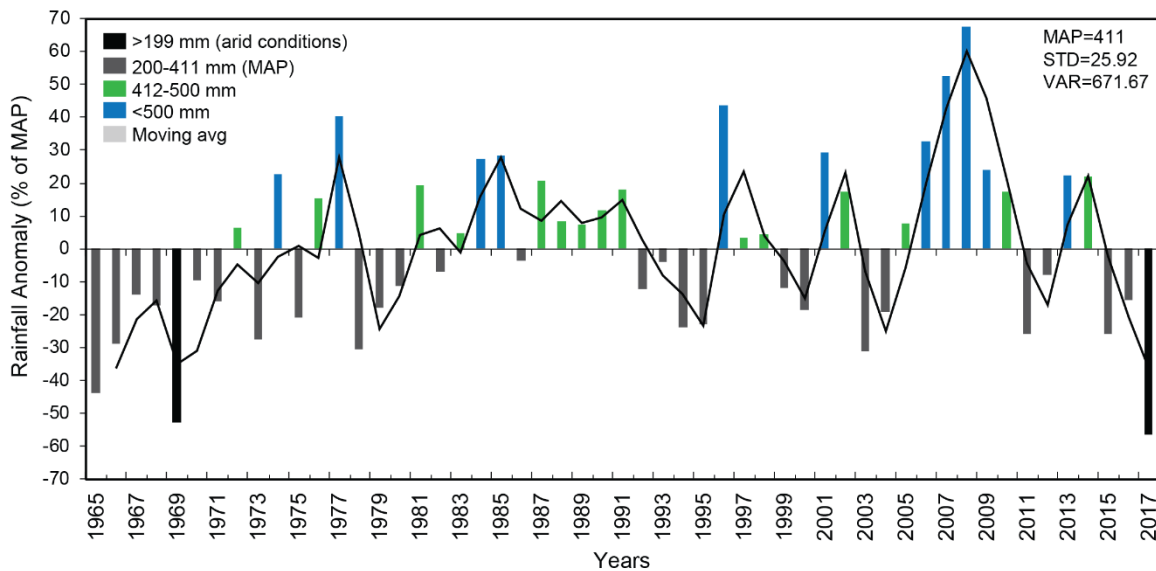
161

162 Figure 3: The difference between MAP and measured rainfall (plotted as rainfall anomaly) for

163 52 years (1965-2017) at location KK-R in the valley of Krom Antonies (after Watson *et al.,*

164 *2018*).

165 While rainfall varies greatly between years in the sub-catchment, it is also spatially impacted

166 by elevational differences. The catchment valley which receives the least MAP 100-350 mm.yr^{-}

167 ^{1} (Lynch, 2004), is between 0-350 masl and is comprised of quaternary sediments that vary in

168 texture, although the majority of the sediments in the sub-catchment are sandy in nature. The

169   higher relief mountainous regions of the sub-catchment between 400-1300 masl receive the

170   highest MAP 400-800 mm.yr^{-1} (Lynch, 2004), are mainly comprised of fractured TMG

171   sandstones, (youngest to oldest): Peninsula, Graafwater (not shown), and Piekernerskloof

172   formations (Fig. 2) (Johnson et al., 2006). Underlying the sandstones and quaternary sediments

173   are the MG shales, which are comprised of the Mooresberg, Piketberg and Klipheuwel

174   formations (Fig. 2) (Rozendaal and Gresse, 1994). Agriculture is the dominant water user in

175   the sub-catchment with an estimated usage of 20 % of the total recharge (Conrad et al., 2004;

176   DWAF, 2003), with the main food crop being potatoes. The MG shales and quaternary

177   sediments, which host the secondary and primary aquifer respectfully, are frequently used to

178   supplement irrigation during the summer months of the year. During winter, the majority of

179   the irrigation water needed for crop growth is supplied by the sub-catchment tributaries or the

180   lake itself. The impact of irrigation on the lake is still regarded as minimal (Meinhardt et al.,

181   2018) but further investigation is still required. For additional information regarding the study

182   site refer to Watson *et al.*, (2018) and Conrad *et al.*, (2004).

183   **3. Methodology**

184   In this study, the J2000 coding was adapted to incorporate distributed groundwater components

185   for the model HRU's (Fig. 4). This was done by aligning the MODFLOW recharge estimates

186   and previous studies (Conrad et al., 2004; Miller et al., 2017; Vetger, 1995; Weaver and Talma,

187   2005; Wu, 2005) with those of the J2000, through adjustment of aquifer hydraulic conductivity

188   from the MODFLOW groundwater model of Krom Antonies (Watson, 2018) (Fig. 5). The

189   assigned hydraulic conductivity for each geological formation was thereafter transferred across

190   the entire J2000 model of the sub-catchment. The adaption applied to the groundwater

191   components influenced the proportioning of water routed to runoff and baseflow within the

192   J2000 model. To validate the outputs of the model, an empirical mode decomposition (EMD)

193   (Huang et al., 1998) was applied to compute the proportion of variation in discharge timeseries

194   that attributed to a high and low water level change at the sub-catchment outlet. The streamflow

195   estimates were thereafter compared with the lake evaporation demand, to understand the sub-

196   catchment water balance.

197   The J2000 model incorporated distributed climate, soil, landuse and hydrogeological

198   information, with aquifer hydraulic conductivity transferred from MODFLOW as described

199   above (Fig. 4). The measured streamflow was used to both calibrate and validate the model,

200   with the landuse dataset being selected according to the period of measured streamflow.

201   Changes in the recorded lake level were used alongside remote sensing to estimate the lake

202   evaporation rate. The impact of irrigation was not included in the model, as there is not enough

203   information available regarding agricultural water use. This is currently one of the major

204   limitations with the study approach presented here and will be the focus of future work. The

205   HRU delineation, model regionalisation, water balance calculations, lateral and reach routing

206   as well as the lake evaporation procedure are presented. Thereafter the input data for the model,

207   the calibration and validation procedures as well as the EMD protocol used, is described.

208
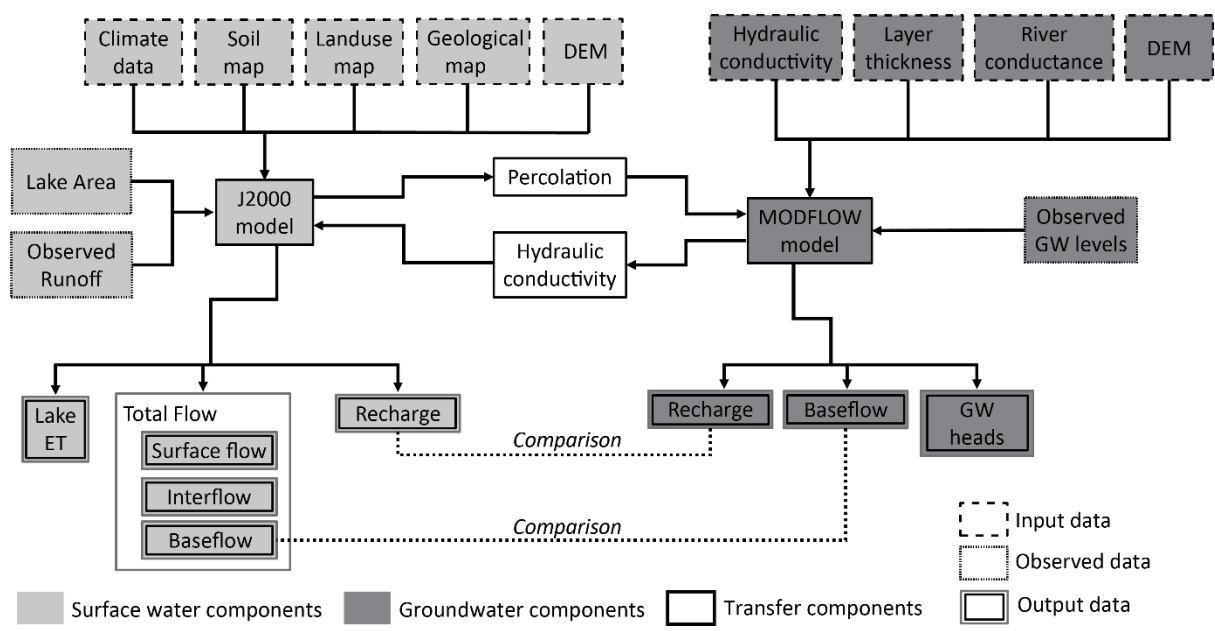
209   Figure 4: Schematic of the model structure, showing the processors simulated by the J2000 and

210   MODFLOW and the components that were transferred from the MODFLOW model
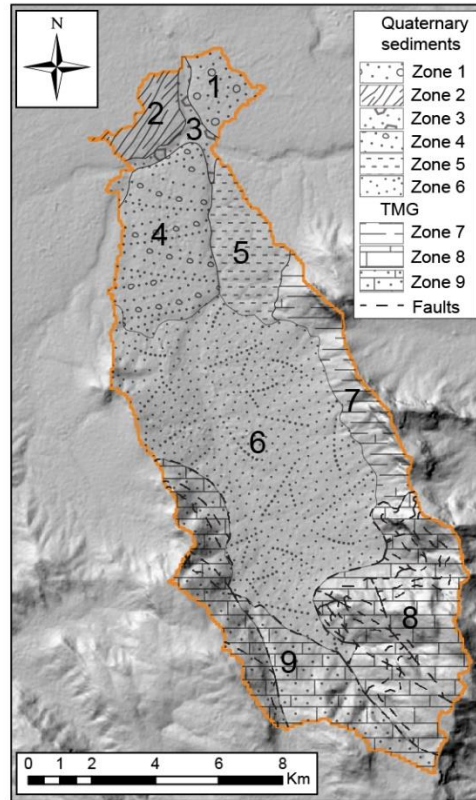
211

212   Figure 5: The aquifer hydraulic zones used for the groundwater calibration of the J2000 (after

213   Watson, 2018)

214   **3.1 Hydrological Response Unit Delineation**

215   HRUs and stream segments (reaches) are used within the J2000 model for distributed

216   topographic and physiological modelling. In this study, the HRU delineation made use of a

217   digital elevation model, with slope, aspect, solar radiation index, mass balance index and

218   topographic wetness being derived. Before the delineation process, gaps within the digital

219   elevation model were filled using a standard fill algorithm from ArcInfo (Jenson and

220   Domingue, 1988). The AML (ArcMarkupLanguage) automated tool (Pfennig et al., 2009) was

221   used for the HRU delineation, with between 13 and 14 HRUs/km^2 being defined

222 (Pfannschmidt, 2008). After the delineation of HRUs, dominant soil, land use and geology

223 properties were assigned to each. The hydrological topology was defined for each HRU by

224 identifying the adjacent HRUs or stream segments that received water fluxes.

225 **3.2 Model regionalisation**

226 Rainfall and relative humidity are the two main parameters that are regionalised within the

227 J2000 model. While a direct regionalisation using an inverse-distance method (IDW) and the

228 elevation of each HRU can be applied to rainfall data, the regionalisation of relative humidity

229 requires the calculation of absolute humidity. The regionalisation of rainfall records was

230 applied by defining the number of weather station records available and estimating the

231 influence on the rainfall amount for each HRU. A weighting for each station using the distance

232 of each station to the area of interest was applied to each rainfall record, using an elevation

233 correction factor (Krause, 2001). The relative humidity and air temperature measured at set

234 weather stations was used to calculate the absolute humidity. Absolute humidity was thereafter

235 regionalised using the IDW method, station and HRU elevation. After the regionalisation had

236 been applied, the absolute humidity was converted back to relative humidity through

237 calculation of saturated vapor pressure and the maximum humidity.

238 **3.3 Water balance calculations**

239 The J2000 model is divided into calculations that impact surface water and groundwater

240 processors. The J2000 model distributes the regionalised precipitation (P) calculated for each

241 HRU using a water balance defined as:

$$P = R + Int_{max} + ETR + \Delta Soil_{sat} \tag{1}$$

242 where R is runoff (mm) (RD1 - surface runoff; RD2 - interflow), Int_{max} is vegetation canopy

243 interception (mm), ETR is 'real' evapotranspiration and $\Delta Soil_{sat}$ is change in soil saturation.

244 The surface water processes have an impact on the amount of modelled runoff and interflow,

245 while the groundwater processors influence the upper and lower groundwater flow

246 components.

247 *3.3.1 Surface water components*

248 Potential evaporation (ETP) within the J2000 model is calculated using the Penman Monteith

249 equation. Before evaporation was calculated for each HRU, interception was subtracted from

250 precipitation using the leaf area index and leaf storage capacity for vegetation (a_rain)

251 (Supplementary: Table 1). Evaporation within the model considers several variables that

252 influence the overall modelled evaporation. Firstly, evaporation is influenced by a slope factor,

253 which was used to reduce ETP based on a linear function. Secondly, the model assumed that

254 vegetation transpires until a particular soil moisture content where ETP is reached, after which

255 modelled evaporation was reduced proportionally to the ETP, until it becomes zero at the

256 permanent wilting point.

257 The soil module in the J2000 model is divided up into processing and storage units. Processing

258 units in the soil module include soil-water infiltration and evapotranspiration, while storage

259 units include middle pore storage (MPS), large pore storage (LPS) and depression storage. The

260 infiltrated precipitation was calculated using the relative saturation of the soil, and its maximum

261 infiltration rate (SoilMaxInfSummer and SoilMaxInfWinter) (Supplementary: Table 1).

262 Surface runoff was generated when the maximum infiltration threshold was exceeded. The

263 amount of water leaving LPS, which can contribute to recharge, was dependant on soil

264 saturation and the filling of LPS via infiltrated precipitation. Net recharge (R_{net}) was estimated

265 using the hydraulic conductivity ($SoilMaxPerc$), the outflow from LPS (LPS_{out}) and the slope

266 ($slope$) of the HRU according to:

$$R_{net} = LPS_{out} \times (1 - \tan (slope)\, SoilMaxPerc) \tag{2}$$

267   The hydraulic conductivity, $SoilMaxPerc$ and the adjusted LPS_{out}.were thereafter used to

268   calculate interflow (IT_f) according to:

$$IT_f = LPS_{out} \times (\tan(slope)\ SoilMaxPerc) \tag{3}$$

269   with the interflow calculated representing the sub-surface runoff component RD2 and is routed

270   as runoff within the model.

271   ***3.3.2 Groundwater components***

272   The J2000 model for the Verlorenvlei sub-catchment was set up with two different geological

273   reservoirs: (1) the primary aquifer (upper groundwater reservoir - RG1), which consists of

274   quaternary sediments with a high permeability; and (2) the secondary aquifer (lower

275   groundwater reservoir- RG2), made up of MG shales and TMG sandstones (Table 1).

Aquifer	Formation	Type	RG1_max (mm)	RG2_max (mm)	RG1_k (d)	RG2_k (d)	RG1_active (n/a)	Kf_geo (mm/d)	depthRG1 (cm)
Primary	Quarternary Sediments	Sediments	50	700	100	431	1	500	1750
Secondary/MG	Moorresberg Formation	Shale Greywacke	0	580	0	350	0	950	1750
Secondary/MG	Porterville Formation	Shale Greywacke	0	560	0	335	0	2	1750
Secondary/MG	Piketberg Formation	Shale Greywacke	0	1000	0	600	0	950	1750
Secondary/MG	Klipheuwel Group	Shale Greywacke	0	500	0	300	0	950	1750
Secondary/TMG	Peninsula Formation	Sandstone	0	1000	0	600	0	950	1750
Secondary/TMG	Piekenierskloof Formation	Sandstone	0	600	0	400	0	1	1750

276

277   Table 1: The J2000 hydrogeological parameters RG1_max, RG2_max, RG1_k, RG2_Kf_geo

278   and depthRG1 assigned to the primary and secondary aquifer formations for the Verlorenvlei

279   sub-catchment

280   The model therefore considered two baseflow components, a fast one from RG1 and a slower

281   one from RG2. The filling of the groundwater reservoirs was done by net recharge, with

282   emptying of the reservoirs possible by lateral subterranean runoff as well as capillary action in

283   the unsaturated zone. Each groundwater reservoir was parameterised separately using the

284   maximum storage capacity (maxRG1 and maxRG2) and the retention coefficients for each

285   reservoir ($recRG1$ and $recRG2$). The outflow from the reservoirs was determined as a function

286   of the actual filling ($actRG1$ and $actRG2$) of the reservoirs and a linear drain function.

287   Calibration parameters $recRG1$ and $recRG2$ are storage residence time parameters. The

288   outflow from each reservoir was defined as:

$$OutRG1 = \frac{1}{gwRG1Fact \times recRG1} \times actRG1 \tag{4}$$

$$OutRG2 = \frac{1}{gwRG2Fact \times recRG2} \times actRG2 \tag{5}$$

289   where $OutRG1$ is the outflow from the upper reservoir, $OutRG2$ is the outflow from the lower

290   reservoir and $gwRG1Fact$/ $gwRG2Fact$ are calibration parameters for the upper and lower

291   reservoir used to determine the outflow from each reservoir. To allocate the quantity of net

292   recharge between the upper (RG1) and lower (RG2) groundwater reservoirs, a calibration

293   coefficient $gwRG1RG2sdist$ was used to distribute the net recharge for each HRU using the

294   HRU slope. The influx of groundwater into the shallow reservoir ($inRG1$) was defined as:

$$inRG1 = R_{net} \times (1 - (1 - \tan(slope))) \times gwRG1RG2sdist \tag{6}$$

295   The influx of net recharge into the lower groundwater reservoir ($inRG2$) was defined as:

$$inRG2 = R_{net} \times (1 - \tan(slope)) \times gwRG1RG2sdist \tag{7}$$

296   with the combination of $OutRG1$ and $OutRG2$ representing the baseflow component that is

297   routed as an outflow from the model.

298   **3.4 Lateral and reach routing**

299   Lateral routing was responsible for water transfer within the model and included HRU influxes

300   and discharge through routing of cascading HRUs from the upper catchment to the exit stream.

301   HRUs were either able to drain into multiple receiving HRUs or into reach segments, where

302   the topographic ID within the HRU dataset determined the drain order. The reach routing

303   module was used to determine the flow within the channels of the river using the kinematic

304   wave equation and calculations of flow according to Manning and Strickler. The river

305 discharge was determined using the roughness coefficient of the stream (Manning roughness),

306 the slope and width of the river channel and calculations of flow velocity and hydraulic radius

307 calculated during model simulations.

3.5 Calculations of lake evaporation rate

309 The lake evaporation rate was based on the ETP calculated by the J2000 and an estimated lake

310 surface area. The lake was modelled as a unique HRU (water as the land-cover type), with a

311 variable area which was estimated using remote sensing data from Landsat 8 and Sentinel-2

312 and the measured lake water level at G3T001 (Fig. 1). To infill lake surface area when remote

313 sensing data was not available, a relationship was created between the estimated lake's surface

314 area and the measured water level between 2015-2017. Where lake water level data was not

315 available (before 1999), an average long-term monthly value was used for the lake evaporation

316 calculations.

3.6 J2000 Input data

3.6.1 Surface water parameters

319 Climate and rainfall: Rainfall, windspeed, relative humidity, solar radiation and air temperature

320 were monitored by Automated Weather Stations (AWS) within and outside of the study

321 catchment (Fig. 1). Of the climate and rainfall data used during the surface water modelling

322 (Watson et al., 2018), data was sourced from seven AWS's of which four stations were owned

323 by the South African Weather Service (SAWS) and three by the Agricultural Research Council

324 (ARC). Two stations that were installed for the surface water modelling, namely Moutonshoek

325 (M-AWS) and Confluence (CN-AWS) were used for climate and rainfall validation due to their

326 short record length. Additional rainfall data collected by farmers at high elevation at location

327 FF-R and within the middle of the catchment at KK-R were used to improve the climate and

328 rainfall network density.

329   Landuse classification: The vegetation and landuse dataset that was used for the sub-catchment

330   (CSIR, 2009) included five different landuse classes: 1) wetlands and waterbodies, 2)

331   cultivated (temporary, commercial, dryland), 3) shrubland and low fynbos, 4) thicket,

332   bushveld, bush clumps and high fynbos and 5) cultivated (permanent, commercial, irrigated).

333   Each different landuse class was assigned an albedo, root depth and seal grade value based on

334   previous studies (Steudel et al., 2015)(Supplementary: Table 2). The Leaf Area Index (LAI)

335   and vegetation height varies by growing season with different values of each for the particular

336   growing season. While surface resistance of the landuse varied monthly within the model, the

337   values only vary significantly between growing seasons.

338   Soil dataset: The Harmonized World Soil Database (HWSD) v1.2 (Batjes et al., 2012) was the

339   input soil dataset, with nine different soil forms within the sub-catchment (Supplementary:

340   Table 3). Within the HWSD, soil depth, soil texture and granulometry were used to calculate

341   and assign soil parameters within the J2000 model. MPS and LPS which differ in terms of the

342   soil structure and pore size were determined in Watson et al. (2018), using pedotransfer

343   functions within the HYDRUS model (Supplementary: Table 3).

344   Streamflow and water levels: Streamflow, measured at the Department of Water Affairs

345   (DWA) gauging station G3H001 between 1970-2009, at the outlet of Kruismans tributary (Het

346   Kruis) (Fig 1 and 3), was used for surface water calibration. The G3H001 two-stage weir could

347   record a maximum flow rate of 3.68 $m^2.s^{-1}$ due to the capacity limitations of the structure. After

348   2009, the G3H001 structure was decommissioned due to structural damage, although repairs

349   are expected in the near future due to increasing concerns regarding the influx of freshwater

350   into the lake. Water levels measured at the sub-catchment outlet at DWA station G3T001 (Fig

351   1) between 1994 to 2018 were used for EMD filtering.

352 *3.6.2 Groundwater parameters*

353 Net recharge and hydraulic conductivity: The hydraulic conductivity values used for the

354 groundwater component adaptation were collected from detailed MODFLOW modelling of

355 Krom Antonies tributary (Fig. 5) (Watson, 2018). The net recharge and aquifer hydraulic

356 conductivity for Krom Antonies tributary, was estimated through PEST autocalibration using

357 hydraulic conductivities from previous studies (SRK, 2009; UMVOTO-SRK, 2000) and

358 potential recharge estimates (Watson et al., 2018).

359 Hydrogeology: Within the hydrogeological dataset, parameters assigned include maximum

360 storage capacity (RG1 and RG2), storage coefficients (RG1 and RG2), the minimum

361 permeability/maximum percolation (Kf_geo of RG1 and RG2) and depth of the upper

362 groundwater reservoir (depthRG1). The maximum storage capacity was determined using an

363 average thickness of each aquifer and the total number of voids and cavities, where the primary

364 aquifer thickness was assumed to be between 15-20 m (Conrad et al., 2004), and the secondary

365 aquifer between 80-200 m (SRK, 2009). The maximum percolation of the different geological

366 formations was assigned hydraulic conductivities using the groundwater model for Krom

367 Antonies sub-catchment (Watson, 2018). The J2000 geological formations were assigned

368 conductivities to modify the maximum percolation value to ensure internal consistency with

369 recharge values calculated using MODFLOW (Table 1).

370 **3.7 J2000 model calibration**

371 *3.7.1 Model sensitivity*

372 The J2000 sensitivity analysis for Verlorenvlei sub-catchment was presented in Watson *et al*.,

373 (2018) and therefore only a short summary is presented here. In this study, parameters that

374 were used to control the ratio of interflow to percolation were adjusted, which in the J2000

375 model include a slope (SoilLatVertDist) and max percolation value. The sensitivity analysis

376 conducted by Watson *et al.*, (2018) showed that for high flow conditions (E2) (Nash-Sutcliffe

377 efficiency in its standard squared), model outputs are most sensitive to the slope factor, while

378 for low flow conditions (E1) (modified Nash-Sutcliffe efficiency in a linear form) the model

379 outputs were most sensitive to the maximum infiltration rate of the soil (ie. the parameter

380 maxInfiltrationWet) (Supplementary: Figure 1). The max percolation was moderately sensitive

381 during wet and dry conditions, and together with the slope factor, controlled the interflow to

382 percolation proportioning that was calibrated in this study.

383 ### *3.7.2 Surface water calibration*

384 The surface water parameters of the model were calibrated for Kruismans tributary (688 km^2)

385 (Fig. 3) using the gauging data from G3H001 (Fig. 6 and Table 1). The streamflow data used

386 for the calibration was between 1986-1993, with model validation between 1994 to 2007 (Fig.

387 6). This specific calibration period was selected due to the wide range of different runoff

388 conditions experienced at the station, with both low and high flow events being recorded. For

389 the calibration, the modelled discharge was manipulated in the same fashion, with a DT limit

390 (discharge table) of 3.68 m³/s, so that the tributary streamflow behaved as measured discharge.
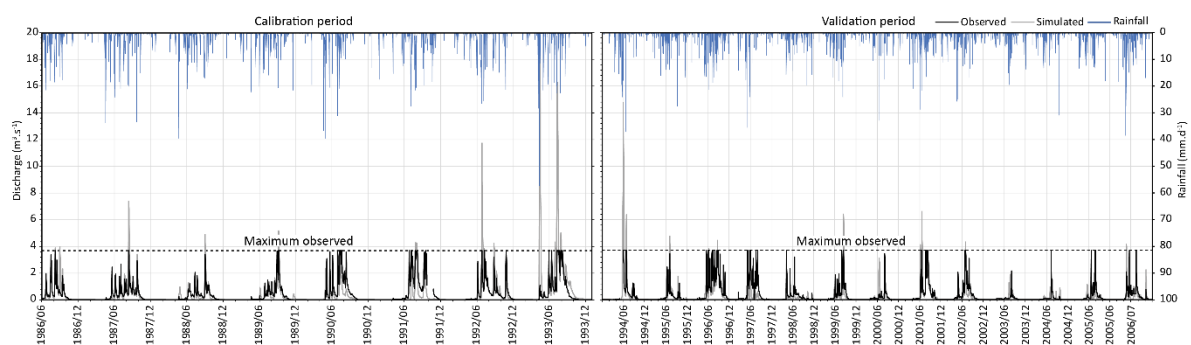
391

392 Figure 6: The surface water calibration (1986-1993) and validation (1994-2006) of the J2000

393 model using gauging data from the G3H001

394 An automated model calibration was performed using the "Nondominating Sorting Genetic

395 Algorithm II" (NSGA-II) multi-objective optimisation method (Deb et al., 2002) with 1024

396   model runs being performed. Narrow ranges of calibration parameters (FC_Adaptation,

397   AC_Adaptation, soilMAXDPS, gwRG1Fact and gwRG2Fact) were chosen to (1) ensure that

398   the modelled recharge from J2000 was within an order of magnitude of recharge from the

399   MODFLOW model and previous studies; (2) achieve a representative sub-catchment

400   hydrograph. As objective functions, Nash-Sutcliffe-Efficiency based on absolute differences

401   (E1) and squared differences 2 (E2) as well as the average bias in % (Pbias) were utilized for

402   the calibration (Krause et al., 2005) (Table 2). The choice of the optimized parameter set was

403   made to ensure that E2 was better than 0.57 (best value was 0.57) and the Pbias better than 5

404   % (Table 1). From the automated calibration, 308 parameter sets were determined with the best

405   E1 being chosen to ensure that the model is representative of low flow conditions (Table 1).

406   ***3.7.3 Model validation***

407   Observed vs modelled streamflow: For the surface water model validation, the streamflow

408   records between 1994-2007 were used, where Nash-Sutcliffe-Efficiency (E1 and E2) were

409   reported. The Pbias was also used as an objective function to report the model performance by

410   comparison between measured and modelled streamflow (Table 2). Although gauging station

411   limitations resulted in good objective functions from the model, the performance of objective

412   functions E1, E2, Pbias reduced between the validation and calibration period (Table 2). During

413   the calibration period there was a good fit between modelled and measured streamflow (Pbias=-

414   1.82), with a significant difference between modelled and measured streamflow during the

415   validation period (Pbias=-19.2). The calibration was performed over a wet cycle (1986-1997),

416   which resulted in a more common occurrence of streamflow events that exceeded 3.68 $m^3.s^{-1}$,

417   thereby reducing the number of calibration points. In contrast the validation was performed

418   over a dry cycle (1997-2007), which resulted in more data points as few streamflow events

419   exceeded 3.68 $m^3.s^{-1}$.

	Calibration 1987-1993	Validation 1994-2007
E1	0.55	0.53
E2	0.57	0.56
LogE1	0.28	0.10
LogE2	0.46	0.19
AVE	-19.24	-269.20
R^2	0.62	0.58
Pbias	-1.82	-19.23758
KGE	0.79	0.67417

420

421 Table 2: Value of the objective functions E1, E2, logarithmic versions of E1 and E2, absolute

422 volume error (AVE), coefficient of determination (R^2), Pbias and Kling Gupta Efficiency

423 (KGE) (Gupta et al., 2009) for surface water calibration (1987-1993) and validation (1994-

424 2007)

425 The J2000 and MODFLOW recharge estimates: With adjustment of hydraulic conductivities

426 from MODFLOW to J2000 it was possible to converge the net recharge estimates between 1.3

427 % with a range of recharge of 0.65-10.03 % for the J2000 and 0.3-11.40 % for MODFLOW.

428 Recharge estimates from previous studies of the primary aquifer indicate recharge rates of 0.2-

429 3.4 % (Conrad et al., 2004), and 8 % Vetger, 1995, while for the TMG aquifer 13 % (Wu,

430 2005), 27 % (Miller et al., 2017) and 17.4 % (Weaver and Talma, 2005) of MAP. J2000

431 estimates had an average value of 5.30 % while MODFLOW was 5.20% for the eight hydraulic

432 zones of Krom Antonies. The coefficient of determination (R^2) between net recharge from the

433 J2000 and MODFLOW was 0.81. Across the entire dataset J2000 overestimated groundwater

434 recharge by 2.75 % relative to MODFLOW, although the coefficient of determination produced

435 an R^2 of 0.92 which is better than during the validation period.

436
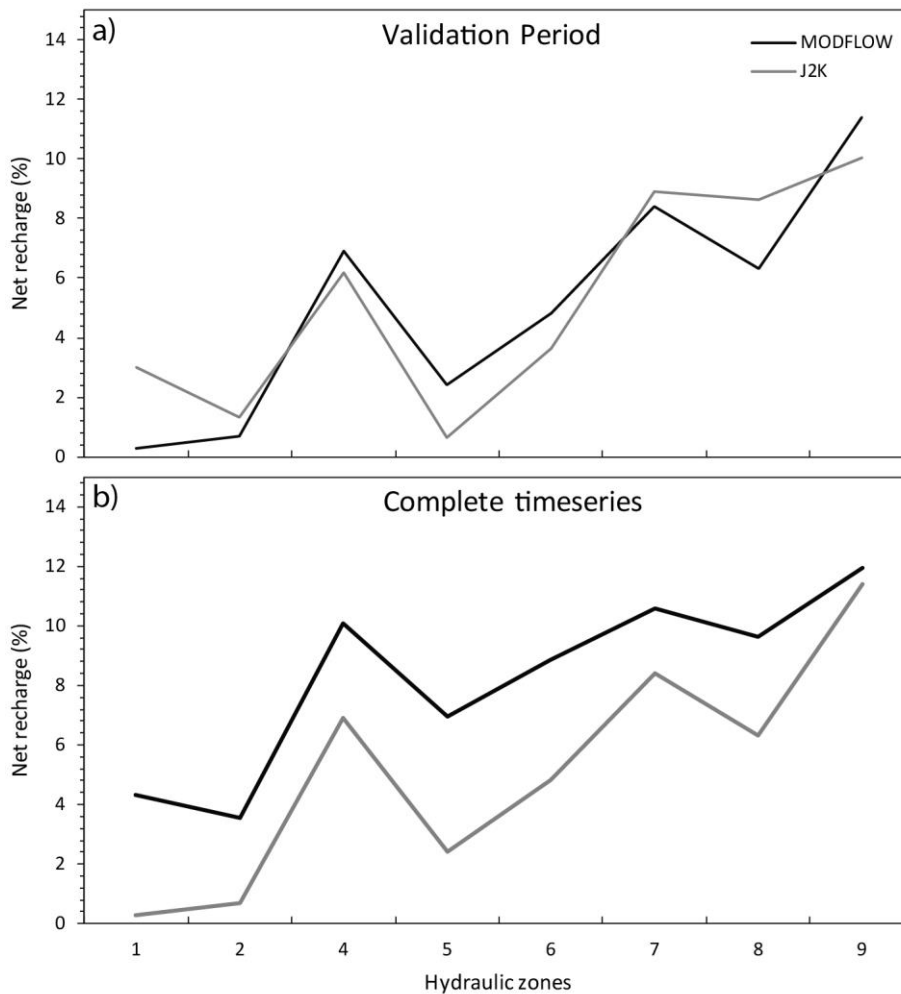
Figure 7: The groundwater calibration for each hydraulic zone with a) net recharge for the

J2000 and MODFLOW during the model calibration (2016) and b) the net recharge deviation

between MODFLOW and J2000 across the entire modelling timestep (1986-2017)

3.8 EMD filtering

To account for missing streamflow data between 2007-2017, an Empirical Mode

Decomposition (EMD) (Huang et al., 1998) was applied to the measured water level data at

the sub-catchment outlet (G3T001)(Fig. 1) between 1994 to 2018 (Fig 8a). EMD is a method

for the decomposition of nonlinear and nonstationary signals into sub-signals of varying

frequency, so-called intrinsic mode functions (IMF), and a residuum signal. By removing one

or more IMF or the residuum signal, certain frequencies (e.g. noise) or an underlying trend can

447   be removed from the original time series data. This approach was successfully applied to the

448   analysis of river runoff data (Huang et al., 2009) and forecasting of hydrological time series

449   (Kisi et al., 2014). In this study, EMD filtering was used to remove high frequency sub-signals

450   from simulated runoff and measured water level data to compare the more general seasonal

451   variations of both signals (Fig. 8b).
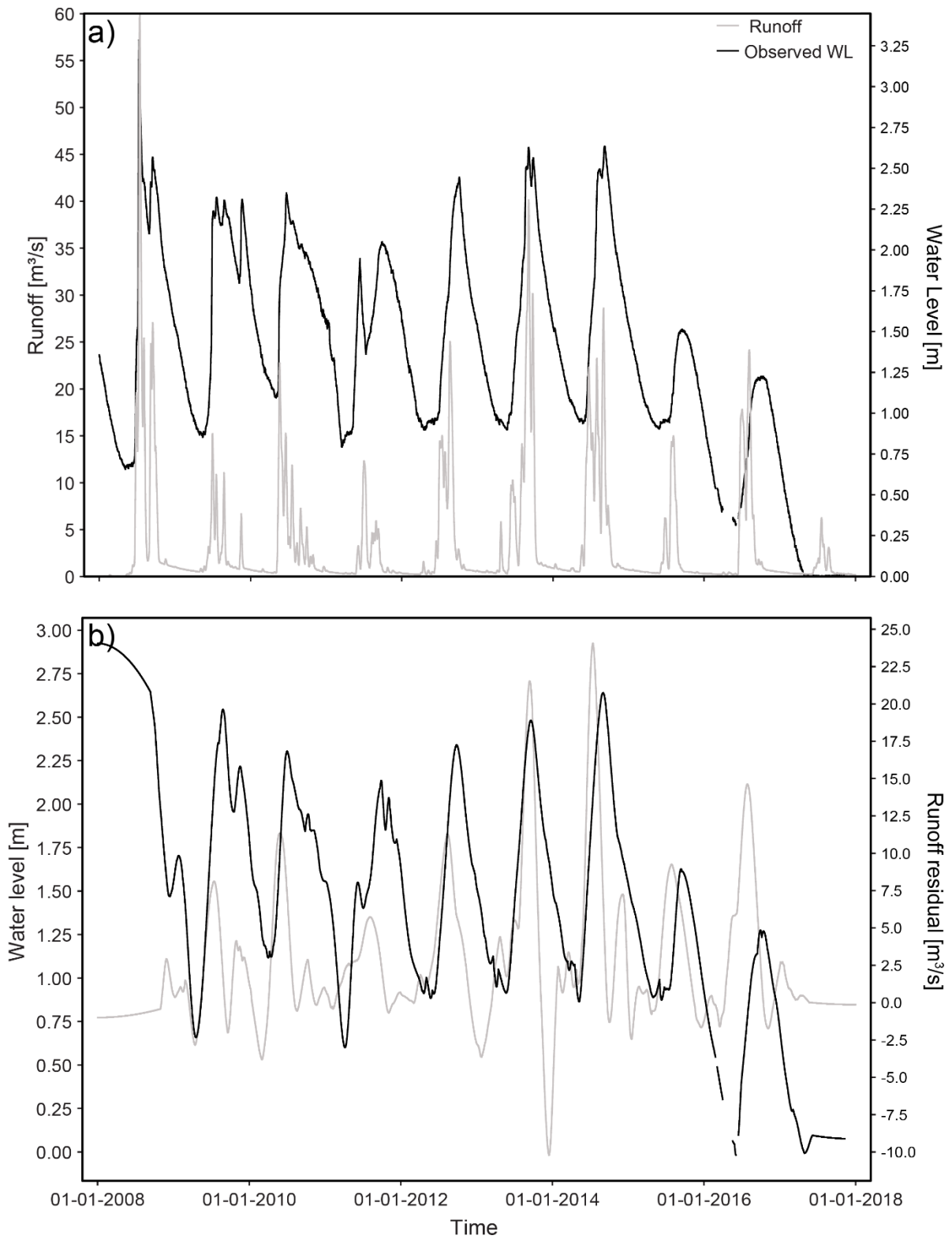
Figure 8: a) The water level fluctuations at station G3T001 with modelled runoff and b) the EMD filtering showing the variation in discharge timeseries attributed a water level change at the station

4. Results

The J2000 model was used to simulate both runoff and baseflow, with runoff being comprised of direct surface runoff (RD1) and interflow (RD2) and baseflow simulated from the primary (RG1) and secondary aquifer (RG2). Below, the results of the modelled streamflow and baseflow are presented, along with the total flow contribution of each tributary, the runoff to baseflow proportioning and stream exceedance probabilities. The coefficient of variation (CV) was used to determine the streamflow variability of each tributary, while the baseflow index (BFI) was used to determine the baseflow and runoff proportion.

4.1 Streamflow and baseflow

Streamflow for the sub-catchment shows two distinctively wet periods (1987-1996 and 2008-2017), separated by a dry period (1997-2007) (Fig. 9). Yearly sub-catchment rainfall volumes between 1987-1996 were between 288 and 492 mm/yr^{-1}, with an average of 426 mm.yr^{-1} and standard deviation (STD) of 51 mm.yr^{-1}. For this period, average yearly streamflow was 1.4 m^3.s-^{1}, with an average baseflow contribution of 0.63 m^3.s^{-1}. The modelled streamflow reached a maximum of 48 m^3.s^{-1} in 1993, where 5 m^3.s^{-1} of baseflow was generated after 58 mm of rainfall was received. Between 1997-2007 (dry period) sub-catchment yearly rainfall was between 222 and 394 mm/yr-^{1} with an average of 326 mm.yr^{-1} and STD of 69 mm.yr^{-1} (Fig. 9). For this same period, average yearly streamflow was 0.44 m^3.s^{-1}, with an average baseflow contribution of 0.18 m^3.s^{-1}. The modelled streamflow reached a maximum of 11 m^3.s^{-1} in 2002, with a baseflow contribution of 2.5 m^3.s^{-1} after 28 mm of rainfall was received. During the second wet period between 2008-2017 sub-catchment yearly rainfall was between 231 and 582 mm.yr^{-1} with an average of 442 mm.yr^{-1} and STD of 112 mm.yr^{-1} (Fig. 9). Over this same period, average yearly streamflow was 2.5 m^3.s^{-1} with an average baseflow contribution of 1.3

479     $m^3.s^{-1}$. The modelled streamflow reached a maximum of 52 $m^3.s^{-1}$ in 2008, with 13 $m^3.s^{-1}$ of

480   baseflow generated after two consecutive rainfall events each of 25 mm.
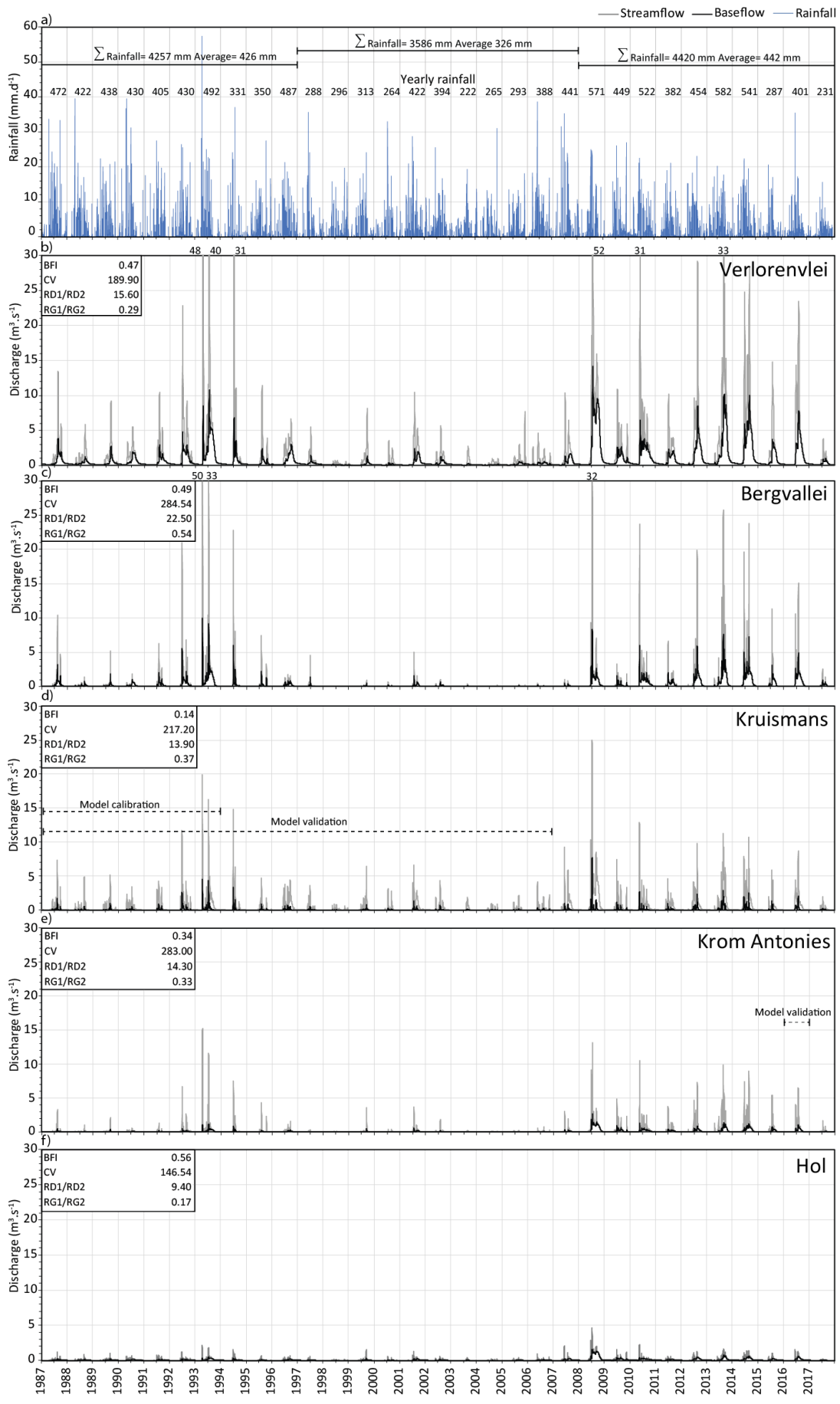
482   Figure 9: a) Average sub-catchment rainfall between 1987-2017 showing wet cycles (1987-

483   1997 and 2008-2017) and dry cycle (1997-2007), Modelled streamflow and baseflow inflows

484   for the b) Verlorenvlei, c) Bergvallei, d) Kruismans, e) Krom Antonies and f) Hol tributaries

485   with estimated BFI, CV, RD1/RD2, RG1/RG2

486   **4.2 Tributary contributions**

487   The four main feeding tributaries (Bergvallei, Kruismans, Hol and Krom Antonies) together

488   contribute 81 % of streamflow for the Verlorenvlei, with the additional 19 % from small

489   tributaries near Redelinghuys (Fig. 10). Kruismans contributes most of the total streamflow at

490   32 %, but only 15 % of the area-weighted contribution as its sub-catchment is the largest of the

491   four tributaries at 688 km^2 (Fig. 10). Bergvallei with a sub-catchment of 320 km^2, contributes

492   29 % of the total flow with an area weighted contribution of 28 %. Krom Antonies has the

493   largest area weighted contribution of 30 % due to its small size (140 km^2) in comparison to the

494   other tributaries, although Krom Antonies contributes only 13 % of the total flow (Fig. 10).

495   Hol sub-catchment at 126 km^2 makes up the smallest contribution to the total flow of only 7

496   %, but has a weighted contribution of 17 % (Fig. 10).

497
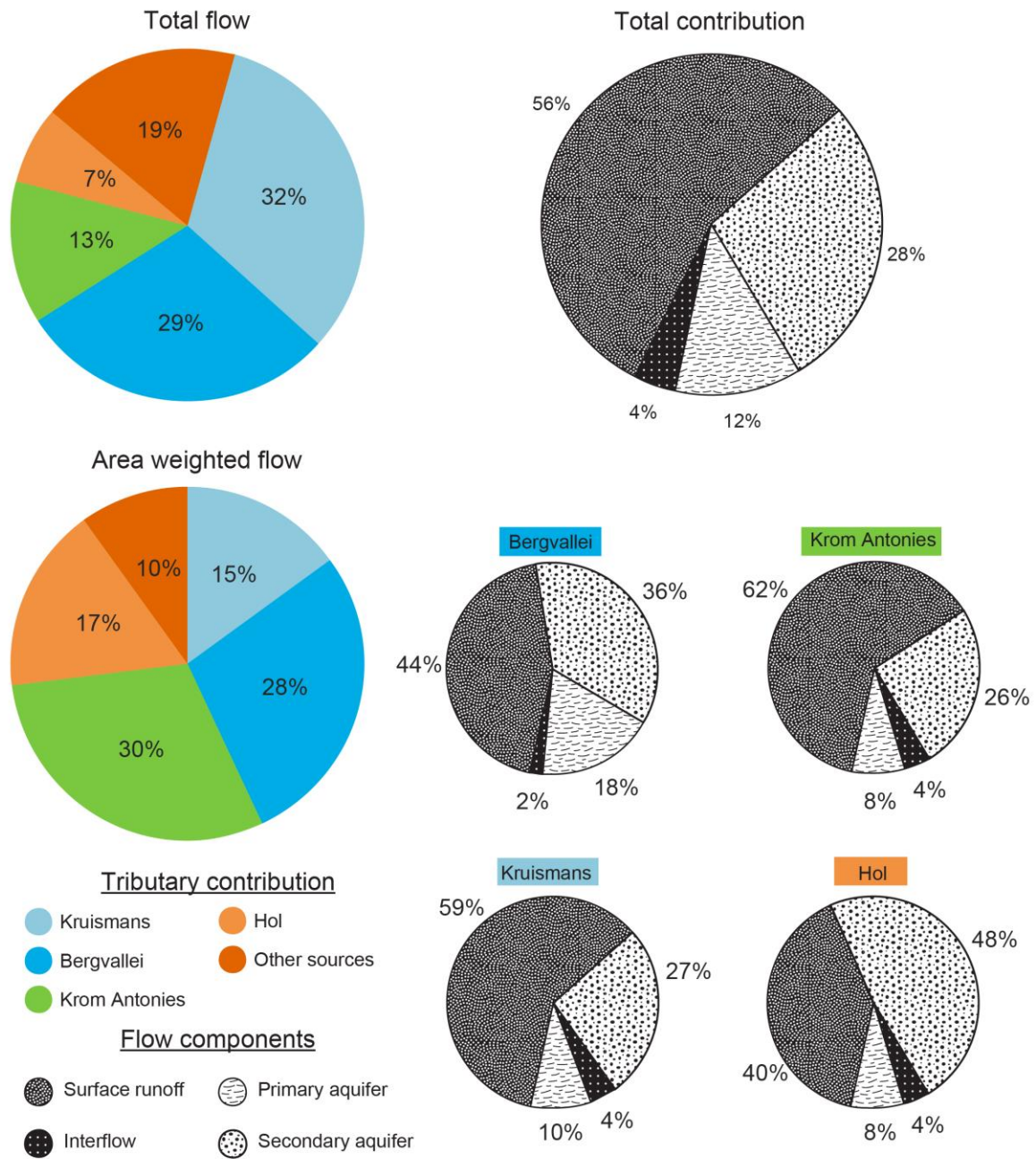
Figure 10: The Verlorenvlei reserve flow contributions (total flow and area weighted flow) of

Kruismans, Bergvallei, Krom Antonies and Hol as well as flow component separation into

surface runoff (RD1), interflow (RD2), primary aquifer flow (RG1) and secondary aquifer

flow (RG2).

4.3 Flow variability

Streamflow that enters Verlorenvlei has a large daily variability with a coefficient of variation (CV) of 189.90 (Fig. 9). This is mainly due to high streamflow variability from Kruismans (32 %) with a CV of 217.20, which is the major total flow contributor (Fig 10). Bergvallei and Krom Antonies, which both have high streamflow variability with CV values of 284.54 and 283.00 respectfully (Fig. 9), further contribute to the high variability of streamflow that enters the lake. While Hol reduces the overall streamflow variability with a CV of 146.54, it is a minor total flow contributor (7 %) and therefore does not reduce the overall streamflow variability significantly (Fig. 10).

Streamflow that enters Verlorenvlei is dominated by surface runoff which makes up 56 % of total flow, with groundwater and interflow contributing 40 % and 4 % respectfully (Fig. 10). The large surface runoff dominance in streamflow entering the lake, is due to a high surface runoff contribution from Kruismans and Krom Antonies, which contribute 26 % of total flow from surface runoff. However, for Bergvallei and Hol, surface runoff contributions are less dominant with 16 % of the total, while the total groundwater contribution is 20 % from these tributaries. Across all four tributaries, the secondary aquifer is the dominant baseflow component with 28 % of total flow, with the primary aquifer contributing 12 %. Bergvallei and Kruismans contribute the majority of primary aquifer baseflow with 8 % of the total. The secondary aquifer baseflow is mainly contributed by Kruismans and Bergvallei, where together 18 % of the total is received. Interflow across the four tributaries is uniformly distributed with 0.3 – 1 % of the total flow being contributed from each tributary.

4.4 Flow exceedance probabilities

The flow exceedance probability, which is a measure of how often a given flow is equalled or exceeded was calculated for each of the tributaries as well as the lake water body. The results

526 for the flow exceedance probabilities includes flow volumes which are exceeded 95 %, 75 %,

527 50 %, 25 % and 5 % of the time. The 95 percentile corresponds to a lake inflow of 0.054 $m^3.s^{-1}$

528 ^{1} or 4,702 $m^3.d^{-1}$, with between 0.001-0.004 $m^3.s^{-1}$ from the feeding tributaries (Fig. 11 and

529 Table 3). The 75-percentile flow, which is exceeded 3/4 of the time corresponds to an inflow

530 of 0.119 $m^3.s^{-1}$ or 10,303 $m^3.d^{-1}$, with between 0.005-0.015 $m^3.s^{-1}$ from the feeding tributaries.

531 Average (50 percentile) streamflow flowing into the Verlorenvlei is 0.237 $m^3.s^{-1}$ or 20,498

532 $m^3.d^{-1}$, with between 0.010-0.035 $m^3.s^{-1}$ from the feeding tributaries. The 25-percentile flow,

533 which is exceeded ¼ of the time corresponds to a lake inflow of 1,067 $m^3.s^{-1}$ or 92,204 $m^3.d^{-1}$

534 with between 0.044-0.291 $m^3.s^{-1}$ from the feeding tributaries. The lake inflows that are

535 exceeded 5 % of the time correspond to 6.939 $m^3.s^{-1}$ or 599,535 $m^3.d^{-1}$ with between 0.224-

536 2.49 $m^3.s^{-1}$ from the feeding tributaries.
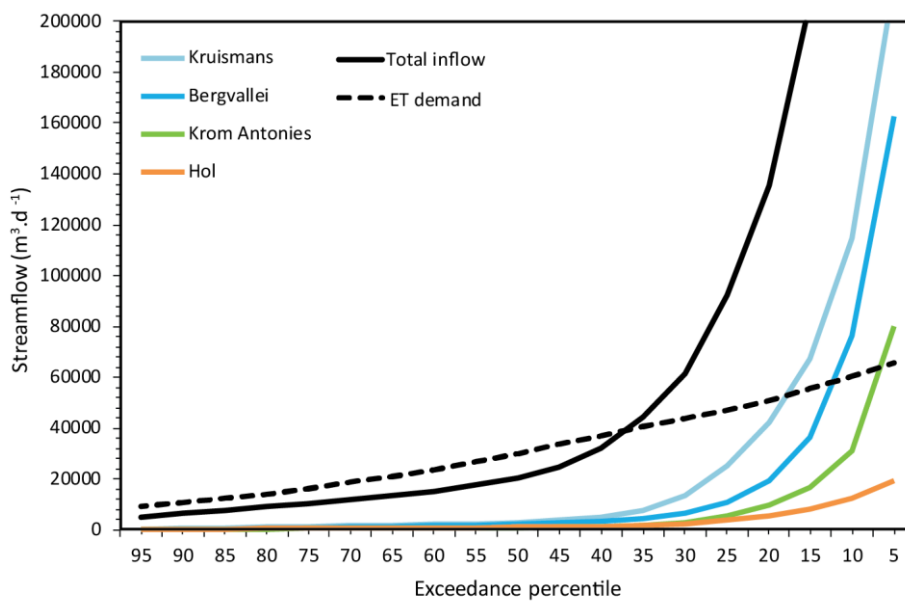
537

538 Figure 11: The streamflow exceedance percentiles and evaporation demand of the Verlorenvlei

539 reserve, with the contributions from each feeding tributary

Exceedance percentile	Lake ET m³.d⁻¹	Verlorenvlei m³.s⁻¹	Verlorenvlei m³.d⁻¹	Kruismans m³.s⁻¹	Kruismans m³.d⁻¹	Bergvallei m³.s⁻¹	Bergvallei m³.d⁻¹	Krom Antonies m³.s⁻¹	Krom Antonies m³.d⁻¹	Hol m³.s⁻¹	Hol m³.d⁻¹
95	9158	0.054	4702	0.004	346	0.001	69	0.001	109	0.002	176
90	10956	0.074	6356	0.007	604	0.002	191	0.003	232	0.003	269
85	12559	0.088	7628	0.010	830	0.004	366	0.004	319	0.004	353
80	14249	0.104	8979	0.012	1072	0.007	596	0.005	392	0.005	434
75	16330	0.119	10303	0.015	1291	0.010	839	0.005	459	0.006	508
70	18653	0.136	11759	0.018	1517	0.013	1104	0.006	534	0.007	587
65	21152	0.155	13373	0.021	1791	0.016	1381	0.007	602	0.008	676
60	23791	0.176	15180	0.024	2104	0.019	1657	0.008	685	0.009	786
55	26979	0.203	17575	0.029	2506	0.023	1965	0.009	772	0.011	913
50	30057	0.237	20498	0.035	3032	0.027	2309	0.010	882	0.012	1058
45	33467	0.286	24669	0.043	3755	0.032	2807	0.012	1024	0.014	1222
40	36760	0.371	32023	0.058	5022	0.041	3511	0.015	1258	0.017	1439
35	40391	0.516	**44598**	0.089	7699	0.053	4613	0.020	1745	0.021	1790
30	43814	0.710	61310	0.156	13511	0.076	6599	0.033	2824	0.029	2481
25	47062	1.067	92204	0.291	25182	0.123	10619	0.062	5387	0.044	3814
20	50997	1.571	135726	0.489	42242	0.223	19295	0.110	9511	0.065	5655
15	55797	2.399	207275	0.780	**67408**	0.421	36354	0.192	16594	0.096	8262
10	60162	3.759	324746	1.324	114432	0.885	**76477**	0.359	31045	0.141	12191
5	65418	6.939	599535	2.490	215152	1.884	162795	0.929	**80305**	0.224	19312

540

Table 3: The streamflow exceedance percentiles and lake evaporation demand for the Verlorenvlei reserve, with the contributions from Kruismans, Bergvallei, Krom Antonies and Hol (m³.s⁻¹ and m³.d⁻¹)

5. Discussion

The adaptation of the J2000 rainfall/runoff model was used to understand the flow contributions of the main feeding tributaries, the proportioning of baseflow to surface runoff as well as how often the inflows exceed the lake evaporation demand. Before a comparison with previous baseflow estimates can be made and the impact of evaporation on the lake reserve, the model limitations and catchment flow dynamics must also be assessed.

5.1 Model limitations and performance

A major limitation facing the development and construction of comprehensive modelling systems in sub-Saharan Africa is the availability of appropriate climate and streamflow data. For this study, while there was access to over 20 years of streamflow records, the station was

554   only able to measure a maximum of 3.68 m³.s⁻¹, which hindered calibration of the model for

555   high flow events. As such, the confidence in the model's ability to simulate high streamflow

556   events using climate records is limited. While the availability of measured data is a limitation

557   that could affect the modelled streamflow, discontinuous climate records also hindered the

558   estimations of long time series streamflow.

559   Over the course of the 31-year modelling period, a number of climate stations used for

560   regionalisation were decommissioned and were replaced by stations in different areas. This

561   required adaption of climate regionalisation for simulations over the entire 31-year period to

562   incorporate the measured streamflow from the gauging station. To account for missing

563   streamflow records since 2007, an EMD filtering protocol was applied to the runoff data (Fig.

564   6). The results from the EMD filtering showed that after removing the first nine IMFs, the local

565   maxima of both signals match the seasonal water level maxima during most of the years. While

566   considerable improvement can be made to the EMD filtering, the results show some agreement

567   which suggested that the simulated runoff was representative of inflows into the lake.

568   **5.2 Catchment dynamics**

569   Factors that impact streamflow variability are important for understanding river flow regime

570   dynamics. Previously, factors that affected streamflow variability such as CV and BFI values

571   were used to determine how susceptible particular river systems were to drought (e.g Hughes

572   and Hannart, 2003). While CV values have been used to account for climatic impacts such as

573   dry and wet cycles, BFI values are associated with runoff generation processes that impact the

574   catchment. For most river systems, BFI values are generally below 1 implying that runoff

575   exceeds baseflow. In comparison CV values can be in excess of 10 implying high variability

576   in streamflow volumes (Hughes and Hannart, 2003). In this study, these two measurements

577   have been applied to tributaries as opposed to quaternary river systems, to understand the

578   streamflow input variability into the Verlorenvlei.

579   The highest proportion of streamflow needed to sustain the Verlorenvlei lake water level is

580   received from the Bergvallei tributary, although the area weighted contribution from Krom

581   Antonies is more significant (Fig. 10). However, CV values for the Bergvallei indicate high

582   streamflow variability. This is partially due to the high surface runoff component in modelled

583   streamflow within the Bergvallei in comparison to the minor interflow contribution, suggesting

584   little sub-surface runoff. While streamflow from the Bergvallei tributary is 54 % groundwater,

585   which would suggest a more sustained streamflow, due to the TMG dominance as well as a

586   high primary aquifer contribution, baseflow from the Bergvallei is driven by highly conductive

587   rock and sediment materials. Similarly, CV values for Krom Antonies indicate high streamflow

588   variability due to the presence of a high baseflow contribution from the conductive TMG and

589   primary aquifers. Although Krom Antonies has a larger interflow component, which would

590   reduce streamflow variability, the dominant TMG presence within this tributary partially

591   compensates for the subsurface flow contributions.

592   In contrast, Hol has a much smaller daily streamflow variability in comparison to both

593   Bergvallei and Krom Antonies (Fig. 9). While streamflow from Hol tributary is mainly

594   comprised of baseflow (56 %), the dominance of low conductive shale rock formations as well

595   as a large interflow component results in reduced streamflow variability. While the larger shale

596   dominance in this tributary not only results in a more sustained baseflow from the secondary

597   aquifer, it also results in a large interflow component due to the limited conductivity of the

598   shale formations. Compounding the more sustained baseflow from Hol tributary, the reduced

599   extent of the primary aquifer results in a dominance in slow groundwater flow from this

600   tributary. Similarly, Kruismans is dominated by shale formations which result in a larger

601 interflow contribution, although due to the limited baseflow contribution (37 %) the streamflow

602 from this tributary is highly variable, which impacts on its susceptibility to drought.

603 The results from this study have shown that while Krom Antonies was initially believed to be

604 the major flow contributor, Bergvallei is in fact the most significant, although streamflow from

605 the four tributaries is highly variable, with baseflow from Hol tributary the only constant input

606 source. The presence of conductive TMG sandstones and quaternary sediments in both Krom

607 Antonies and Bergvallei, results in quick baseflow responses with little flow attenuation. The

608 potential implication of a constant source of groundwater being provided from Hol tributary,

609 is that if the groundwater is of poor quality this would result in a constant input of saline

610 groundwater, with Krom Antonies and Bergvallei providing freshwater only after sufficient

611 rainfall has been received.

612 **5.3 Baseflow comparison**

613 The groundwater components of the J2000 model were adjusted using aquifer hydraulic

614 conductivity from a MODFLOW model of one of the main feeding tributaries of the

615 Verlorenvlei. Krom Antonies was selected as it was previously believed to be the largest input

616 of groundwater to Verlorenvlei (Fig. 2). Baseflow for Krom Antonies tributary was previously

617 calculated using a MODFLOW model (Watson, 2018), by considering aquifer hydraulic

618 conductivity and average groundwater recharge. As average recharge was used, baseflow

619 estimates from MODFLOW are likely to fall on the upper end of daily baseflow values

620 estimated by the J2000 model. For Krom Antonies sub-catchment, Watson, (2018) estimated

621 baseflow between 14,000 to 19,000 $m^3.d^{-1}$ for 2010-2016 using MODFLOW. Similar daily

622 baseflow estimates from the J2000 were only exceeded 10 % of the time, with average

623 estimates (50 %) of 1,036 $m^3.d^{-1}$ over the course of the modelling period (Fig. 9).

624 The MODFLOW estimates were applied over the course of a wet cycle (2016). In comparison

625 to the MODFLOW estimates (14,000 to 19,000 $m^3.d^{-1}$) average baseflow from J2000 for 2016

626 was 8, 214 $m^3.d^{-1}$. The daily timestep nature of the J2000 is likely to result in far lower baseflow

627 estimates, as recharge is only received over a 6-month period as opposed to a yearly average

628 estimate. One possible implication of this is that while common groundwater abstraction

629 scenarios have been based on yearly recharge, abstraction is likely to exceed sustainable

630 volumes during dry months or dry cycles and this could hinder the ability of the aquifer to

631 supply baseflow. While the groundwater components of the J2000 have been distributed to

632 allow for improved baseflow estimates, the groundwater calibration was applied to Krom

633 Antonies. However, this study showed that Bergvallei has been identified as the largest water

634 contributor. In hindsight, the use of geochemistry to identify dominant tributaries could have

635 aided the groundwater model adaption. While it would have been beneficial to adapt the

636 groundwater components of the J2000 using the dominant baseflow contributor, considering

637 the geological heterogeneity between tributaries is more important for identifying how to adapt

638 the groundwater components of the J2000. While the distribution of aquifer components

639 improved modelled baseflow, including groundwater abstraction scenarios in baseflow

640 modelling in the sub-catchment is important for future water management for this ecologically

641 significant area.

642 **5.4 The Verlorenvlei reserve and the evaporative demand**

643 For this study, exceedance probabilities were estimated through rainfall/runoff modelling for

644 the previous 31 years within the Verlorenvlei sub-catchment. The exceedance probabilities

645 were determined for each tributary, as well as the total inflows into the lake. These exceedance

646 probabilities were compared with the evaporative demand of the lake, to understand whether

647 inflows are in surplus or whether the evaporation demand exceeds inflow.

648 From the exceedance probabilities generated in this study, the lake is predominately fed by less

649 frequent large discharge events, where on average the daily inflows to the lake do not sustain

650 the lake water level. This is particularly evident in the measured water level data from station

651 G3T001, where measured water levels have a large daily standard deviation (0.62) (Watson *et*

652 *al*., 2018). The daily inflows of water into the Verlorenvlei has also been subject to significant

653 rainfall variability, with yearly rainfall between the second wet cycle (2007-2017) being twice

654 as variable in comparison to the first wet cycle (1987-1996). The change in rainfall variability

655 has had a significant impact on soil moisture conditions, resulting in not only larger peak

656 discharges but also lengthened low flow conditions. With climate change likely to impact the

657 length and severity of dry cycles, it is likely that the lake will dry up more frequently into the

658 future, which could have severe implications on the biodiversity that relies on the lake's habitat

659 for survival. Of importance to the lake's survival is the protection of river inflows during wet

660 cycles, where the lake requires these inflows for regeneration.

661 While the impact of irrigation could not be incorporated, over allocation of water resources

662 may potentially have a significant impact on the catchment water balance, especially during

663 wet cycles when ecosystems are recovering from dry conditions. The increased irrigation

664 during wet cycles as a result of agricultural development, could be a further impact on the

665 recovery of sensitive ecosystems. This type of issue is not limited to Verlorenvlei but applies

666 to many wetlands or estuarine lakes around the world, while they have been classified as

667 protected areas, water resources within the catchments are required for food security. As

668 climate change drives increased temperatures and variability in rainfall, the $\pm$ 10-year cycles

669 of dry and wet conditions may no longer be valid anymore, where these conditions may shorten

670 or lengthen. With the routine breaking of weather records across the world (Bruce, 2018; Davis,

671 2018), it is becoming increasingly evident that conditions are changing and becoming more

672   variable, which could impact sensitive ecosystems around the world, highlighting the need for

673   effective water management protocols during times of limited rainfall.

674

6. Conclusion

Understanding river flow regime dynamics is important for the management of ecosystems that are sensitive to streamflow fluctuations. While climatic factors impact rainfall volumes during wet and dry cycles, factors that control catchment runoff and baseflow are key to the implementation of river protection strategies. In this study, groundwater components within the J2000 model were distributed to improve baseflow and runoff proportioning for the Verlorenvlei sub-catchment. The J2000 was distributed using groundwater model values for the dominant baseflow tributary, while calibration was applied to the dominant streamflow tributary. The model calibration was hindered by the DT limit, which reduced the confidence in modelling high flow events, although an EMD filtering protocol was applied to account for the resolution limitations and missing streamflow records. The modelling approach would likely be transferable to other partially gauged semi-arid catchments, provided that groundwater recharge is well constrained. The daily timestep nature of the J2000 model allowed for an in-depth understanding of tributary flow regime dynamics, showing that while streamflow variability is influenced by the runoff to baseflow proportion, the host rock or sediment in which groundwater is held is also a factor that must be considered. The modelling results showed that on average the streamflow influxes were not able to meet the evaporation demand of the lake, with yearly rainfall becoming more variable. High-flow events, although they occur infrequently, are responsible for regeneration of the lake's water level and ecology, which illustrates the importance of wet cycles in maintaining biodiversity levels in semi-arid environments. With climate change likely to impact the length and occurrence of dry cycle conditions, wet cycles become particularly important for ecosystem regeneration, especially for semi-arid regions such as the Verlorenvlei.

7. Acknowledgements

The authors would like to thank the WRC and SASSCAL for project funding as well as the NRF and Iphakade for bursary support. Agricultural Research Council (ARC) and South African Weather Service (SAWS) for their access to climate and rainfall data. The research was carried out in the framework of SASSCAL and was funded by the German Federal Ministry of Education and Research (BMBF) under promotion number 01LG1201E.

8. References

Acreman, M. C. and Dunbar, M. J.: Defining environmental river flow requirements – a review, Hydrol. Earth Syst. Sci., 8(5), 861–876, 2004.

Arnold, J. G., Srinivasan, R., Muttiah, R. S. and Williams, J. R.: Large area hydrologic modeling and assessment Part I: Model development, , 34(1), 73–89, 1998.

Arthington, A. H., Kennen, J. G., Stein, E. D. and Webb, J. A.: Recent advances in environmental flows science and water management — Innovation in the Anthropocene, Freshw. Biol., (March), 1–13, 2018.

Barker, I. and Kirmond, A.: Managing surface water abstraction in Wheater, H. and Kirby, C.(eds) Hydrology in a changing environment, vol1, Br. Hydrol. Soc., 249–258, 1998.

Batjes, N., Dijkshoorn, K., Van Engelen, V., Fischer, G., Jones, A., Montanarella, L., Petri, M., Prieler, S., Teixeira, E. and Wiberg, D.: Harmonized World Soil Database (version 1.2), Tech. rep., FAO and IIASA, Rome, Italy and Laxenburg, Austria., 2012.

Bauer, P., Held, R. J., Zimmermann, S., Linn, F. and Kinzelbach, W.: Coupled flow and salinity transport modelling in semi-arid environments: The Shashe River Valley, Botswana, J. Hydrol., 316(1–4), 163–183, 2006.

720   Bragg, O. M., Black, A. R., Duck, R. W. and Rowan, J. S.: Progress in Physical Geography

721   Approaching the physical-biological interface in rivers : a review of methods, , 4(October

722   2000), 506–531, 2005.

723   Bruce, D.: Prepare for extended severe weather seasons, Aust. J. Emerg. Manag., 33(4), 6,

724   2018.

725   Bunn, S. E. and Arthington, A. H.: Basic principles and ecological consequences of altered

726   flow regimes for aquatic biodiversity, Environ. Manage., 30(4), 492–507, 2002.

727   Conrad, J., Nel, J. and Wentzel, J.: The challenges and implications of assessing groundwater

728   recharge: A case study-northern Sandveld , Western Cape, South Africa, Water SA, 30(5), 75–

729   81, 2004.

730   Costanza, R., Arge, R., Groot, R. De, Farberk, S., Grasso, M., Hannon, B., Limburg, K.,

731   Naeem, S., O'Neill, R. V, Paruelo, J., Raskin, R. G., Suttonkk, P. and van den Belt, M.: The

732   value of the world's ecosystem services and natural capital, Nature, 387, 253–260, 1997.

733   CSIR: Development of the Verlorenvlei estuarine management plan: Situation assessment.

734   Report prepared for the C.A.P.E. Estuaries Programme, , 142, 2009.

735   Davis, G.: The Energy-Water-Climate Nexus and Its Impact on Queensland's Intensive

736   Farming Sector, in The Impact of Climate Change on Our Life, pp. 97–126, Springer., 2018.

737   Deb, K., Pratap, A., Agarwal, S. and Meyarivan, T.: A fast and elitist multiobjective genetic

738   algorithm: NSGA-II, IEEE Trans. Evol. Comput., 6(2), 182–197, 2002.

739   Diersch, H.-J. G.: FEFLOW reference manual, Inst. Water Resour. Plan. Syst. Res. Ltd, 278,

740   2002.

741   Domenico, P. A. and Schwartz, F. W.: Physical and Chemical Hydrogeology, John Wiley and

742   Sons, Inc., New York., 1990.

743   DWAF: Sandveld Preliminary (Rapid) Reserve Determinations. Langvlei, Jakkals and

744   Verlorenvlei Rivers. Olifants-Doorn WMA G30. Surface Volume 1: Final Report Reserve

745   Specifications. DWAF Project Number: 2002-227., 2003.

746   Flügel, W.: Delineating hydrological response units by geographical information system

747   analyses for regional hydrological modelling using PRMS/MMS in the drainage basin of the

748   River Bröl, Germany, Hydrol. Process., 9(3-4), 423–436, 1995.

749   Gleeson, T. and Richter, B.: How much groundwater can we pump and protect environmental

750   flows through time? Presumptive standards for conjunctive management of aquifers and rivers,

751   River Res. Appl., 34, 83–92, doi:10.1002/rra.3185, 2018.

752   Gleick, P. H.: Global freshwater resources: soft-path solutions for the 21st century, Science

753   (80-.)., 302(5650), 1524–1528, 2003.

754   Harbaugh, Arlen, W.: MODFLOW-2005 , The U . S . Geological Survey Modular Ground-

755   Water Model — the Ground-Water Flow Process, U.S. Geol. Surv. Tech. Methods, 253, 2005.

756   Harbaugh, B. A. W., Banta, E. R., Hill, M. C. and Mcdonald, M. G.: MODFLOW-2000 , THE

757   U . S . GEOLOGICAL SURVEY MODULAR GROUND-WATER MODEL — USER

758   GUIDE TO MODULARIZATION CONCEPTS AND THE GROUND-WATER FLOW

759   PROCESS, Reston, Virginia., 2000.

760   Harman, C. and Stewardson, M.: Optimizing dam release rules to meet environmental flow

761   targets, River Res. Appl., 21(2–3), 113–129, 2005.

762   Helme, N.: Botanical report: Fine Scale vegetation mapping in the Sandveld, as part of the

763   C.A.P.E programme., 2007.

764   Huang, N. E., Shen, Z., Long, S. R., Wu, M. C., Shih, H. H., Zheng, Q., Yen, N.-C., Tung, C.

765   C. and Liu, H. H.: The empirical mode decomposition and the Hilbert spectrum for nonlinear

766   and non-stationary time series analysis, in Proceedings of the Royal Society of London A:

767   mathematical, physical and engineering sciences, vol. 454, pp. 903–995, The Royal Society.,

768   1998.

769   Huang, Y., Schmitt, F. G., Lu, Z. and Liu, Y.: Analysis of daily river flow fluctuations using

770   empirical mode decomposition and arbitrary order Hilbert spectral analysis, J. Hydrol., 373(1–

771   2), 103–111, 2009.

772   Hughes, D. A.: Providing hydrological information and data analysis tools for the

773   determination of ecological instream flow requirements for South African rivers, J. Hydrol.,

774   241(1–2), 140–151, 2001.

775   Hughes, D. A. and Hannart, P.: A desktop model used to provide an initial estimate of the

776   ecological instream flow requirements of rivers in South Africa, J. Hydrol., 270(3–4), 167–

777   181, 2003.

778   Jenson, S. K. and Domingue, J. O.: Extracting topographic structure from digital elevation data

779   for geographic information system analysis, Photogramm. Eng. Remote Sensing, 54(11),

780   1593–1600, 1988.

781   Johnson, M. R., Anhauesser, C. R. and Thomas, R. J.: The Geology of South Africa, Geological

782   Society of South Africa., 2006.

783   Kim, N. W., Chung, I. M., Won, Y. S. and Arnold, J. G.: Development and application of the

784   integrated SWAT-MODFLOW model, J. Hydrol., 356(1–2), 1–16, 2008.

785   King, J. and Louw, D.: Instream flow assessments for regulated rivers in South Africa using

786   the Building Block Methodology, Aquat. Ecosyst. Health Manag., 1(2), 109–124, 1998.

787   Kisi, O., Latifoğlu, L. and Latifoğlu, F.: Investigation of empirical mode decomposition in

788   forecasting of hydrological time series, Water Resour. Manag., 28(12), 4045–4057, 2014.

789   Krause, P.: Das hydrologische Modellsystem J2000. Beschreibung und Anwendung in großen

790   Flussgebieten, in Umwelt/Environment, Vol. 29. Jülich: Research centre., 2001.

791   Krause, P., Boyle, D. P. and Bäse, F.: Comparison of different efficiency criteria for

792   hydrological model assessment, Adv. Geosci., 5, 89–97, 2005.

793   Leavesley, G. H. and Stannard, L. G.: Application of remotely sensed data in a distributed-

794   parameter watershed model, in Proceedings of the Workshop on Applications of Remote

795   Sensing in Hydrology, Saskatoon, pp. 47–64., 1990.

796   Lynch, S.: Development of a raster database of annula, monthly and daily rainfall for southern

797   Africa, Pietermaritzburg., 2004.

798   Martens, K., Davies, B. R., Baxter, A. J. and Meadows, M. E.: A contribution to the taxonomy

799   and ecology of the Ostracoda (Crustacea) from Verlorenvlei (Western Cape, South Africa),

800   African Zool., 31(1), 22–36, 1996.

801   Meinhardt, M., Fleischer, M., Fink, M., Kralisch, S., Kenabatho, P., de Clercq, W. P., Zimba,

802   H., Phiri, W. and Helmschrot, J.: Semi-arid catchments under change: Adapted hydrological

803   models to simulate the influence of climate change and human activities on rainfall-runoff

804   processes in southern Africa, in Climate change and adaptive land management in southern

805   Africa – assessments, changes, challenges, and solutions, edited by N. Revermann, R.,

806   Krewenka, K.M., Schmiedel, U., Olwoch, J.M., Helmschrot, J. & Jürgens, pp. 114–130, Klaus

807   Hess Publishers, Göttingen & Windhoek., 2018.

808   Miller, J. A., Dunford, A. J., Swana, K. A., Palcsu, L., Butler, M. and Clarke, C. E.: Stable

809   isotope and noble gas constraints on the source and residence time of spring water from the

Table Mountain Group Aquifer, Paarl, South Africa and implications for large scale abstraction, J. Hydrol., 551, 100–115, 2017.

Muche, G., Kruger, S., Hillman, T., Josenhans, K., Ribeiro, C., Bazibi, M., Seely, M., Nkonde, E., de Clercq, W. P., Strohbach, B., Kenabatho, K. ., Vogt, R., Kaspar, F., Helmschrot, J. and Jürgens, N.: Climate change and adaptive land management in southern Africa – assessments, changes, challenges, and solutions, in Biodiversity & Ecology, edited by R. Revermann, K. M. Krewenka, U. Schmiedel, J. . Olwoch, J. Helmschrot, and N. Jürgens, pp. 34–43, Klaus Hess Publishers, Göttingen & Windhoek., 2018.

Nelson, E., Mendoza, G., Regetz, J., Polasky, S., Tallis, H., Cameron, Dr., Chan, K. M. A., Daily, G. C., Goldstein, J. and Kareiva, P. M.: Modeling multiple ecosystem services, biodiversity conservation, commodity production, and tradeoffs at landscape scales, Front. Ecol. Environ., 7(1), 4–11, 2009.

O'Keeffe, J.: Sustaining river ecosystems: Balancing use and protection, Prog. Phys. Geogr., 33(3), 339–357, 2009.

Olden, J. D. and Naiman, R. J.: Incorporating thermal regimes into environmental flows assessments: Modifying dam operations to restore freshwater ecosystem integrity, Freshw. Biol., 55(1), 86–107, 2010.

Pfannschmidt, K.: Optimierungsmethoden zur HRU-basierten N/A-Modellierung für eine operationelle Hochwasservorhersage auf Basis prognostischer Klimadaten des Deutschen Wetterdienstes: Untersuchungen in einem mesoskaligen Einzugsgebiet im Thüringer Wald, 2008.

Pfennig, B., Kipka, H., Fink, M., Wolf, M., Krause, P. and Flügel, W.-A.: Development of an extended routing scheme in reference to consideration of multi-dimensional flow relations

833   between hydrological model entities, 18th World IMACS / MODSIM Congr. Cairns, Aust. 13-

834   17 July 2009., 2009.

835   Poff, N. L., Allan, J. D., Bain, M. B., Karr, J. R., Prestegaard, K. L., Richter, B. D., Sparks, R.

836   E. and Stromberg, J. C.: A paradigm for river conservation and restoration, Bioscience, 47(11),

837   769–784, 1997.

838   Poff, N. L., Richter, B. D., Arthington, A. H., Bunn, S. E., Naiman, R. J., Kendy, E., Acreman,

839   M., Apse, C., Bledsoe, B. P., Freeman, M. C., Henriksen, J., Jacobson, R. B., Kennen, J. G.,

840   Merritt, D. M., O'Keeffe, J. H., Olden, J. D., Rogers, K., Tharme, R. E. and Warner, A.: The

841   ecological limits of hydrologic alteration (ELOHA): A new framework for developing regional

842   environmental flow standards, Freshw. Biol., 55(1), 147–170, 2010.

843   Postel, S. and Carpenter, S.: Freshwater ecosystem services, Nature's Serv. Soc. Depend. Nat.

844   Ecosyst., 195, 1997.

845   Postel, S. and Richter, B.: Rivers for life: managing water for people and nature, Island Press.,

846   2012.

847   Richter, B. D.: Re-thinking environmental flows: from allocations and reserves to sustainability

848   boundaries, River Res. Appl., 26(8), 1052–1063, 2010.

849   Richter, B. D., Mathews, R., Harrison, D. L. and Wigington, R.: Ecologically sustainable water

850   management: Managing river flows for ecological integrity, Ecol. Appl., 13(1), 206–224, 2003.

851   Richter, B. D., Davis, M. M., Apse, C. and Konrad, C.: A presumptive standard for

852   environmental flow protection, River Res. Appl., 28, 1312–1321, 2012.

853   Ridoutt, B. G. and Pfister, S.: A revised approach to water footprinting to make transparent the

854   impacts of consumption and production on global freshwater scarcity, Glob. Environ. Chang.,

855   20(1), 113–120, 2010.

856   Rozendaal, A. and Gresse, P. G.: Structural setting of the Riviera W-Mo deposit, western Cape,

857   South Africa, South African J. Geol., 97(2), 184, 1994.

858   Sigidi, N. T.: Geochemical and isotopic tracing of salinity loads into the Ramsar listed

859   Verlorenvlei freshwater estuarine lake , Western Cape , South Africa, (Unpublished MSc

860   thesis) Stellenbosch University., 2018.

861   Sinclair, S., Lane, S. and Grindley, J.: Estuaries of the Cape: Part II: Synopses of avaiable

862   information on individual systems., Stellenbosch., 1986.

863   SRK: Preliminary Assessment of Impact of the Proposed Riviera Tungsten Mine on

864   Groundwater Resources Preliminary Assessment of Impact of the Proposed Riviera Tungsten

865   Mine on Groundwater Resources., 2009.

866   Steudel, T., Bugan, R., Kipka, H., Pfennig, B., Fink, M., de Clercq, W., Flügel, W.-A. and

867   Helmschrot, J.: Implementing contour bank farming practices into the J2000 model to improve

868   hydrological and erosion modelling in semi-arid Western Cape Province of South Africa,

869   Hydrol. Res., 46(2), 192, 2015.

870   Tennant, D. L.: Instream Flow Regimens for Fish , Wildlife , Recreation and Related

871   Environmental Resources, Fisheries, 1(4), 6–10, 1976.

872   UMVOTO-SRK: Reconnaissance investigation into the development and utilization of the

873   Table Mountain Group Artesian Groundwater, using the E10 catchment as a pilot study area.,

874   2000.

875   Vetger, J. R.: An explanation of a set of national groundwater maps. WRC report TT 74/95,

876   Water Res. Comm. Pretoria, South Africa, 1995.

877 Wagener, T. and Wheater, H. S.: Parameter estimation and regionalization for continuous

878 rainfall-runoff models including uncertainty, J. Hydrol., 320(1–2), 132–154, 2006.

879 Watson, A. P.: Using distributive surface water and groundwater modelling techniques to

880 quantify groundwater recharge and baseflow for the Verlorenvlei estuarine system , west coast

881 , South Africa, (Unpublished PhD thesis) Stellenbosch University., 2018.

882 Watson, A. P., Miller, J. A., Fleischer, M. and de Clercq, W. P.: Estimation of groundwater

883 recharge via percolation outputs from a rainfall/runoff model for the Verlorenvlei estuarine

884 system, west coast, South Africa., J. Hydrol., 558(C), 238–254, 2018.

885 Weaver, J. and Talma, A.: Cumulative rainfall collectors – A tool for assessing groundwater

886 recharge, , 31(3), 283–290, 2005.

887 Willems, P.: A time series tool to support the multi-criteria performance evaluation of rainfall-

888 runoff models, Environ. Model. Softw., 24(3), 311–321, doi:10.1016/j.envsoft.2008.09.005,

889 2009.

890 Wishart, M. J.: The terrestrial invertebrate fauna of a temporary stream in southern Africa,

891 African Zool., 35(2), 193–200, 2000.

892 Wu, Y.: Groundwater recharge estimation in Table Mountain Group aquifer systems with a

893 case study of Kammanassie area, 2005.

894 Young, A. R.: Stream flow simulation within UK ungauged catchments using a daily rainfall-

895 runoff model, J. Hydrol., 320, 155–172, 2006.

896